Supplementary Materials for "Fractal Geometry of Aerosol Particles and Its Impact on Atmospheric Optical Properties: Development and Validation of the Fractal Aerosol Cluster Model in a Heavy Haze Event"

Liu Zhenxin[1†], Li Weimin[1], Zhang Bihui[2], Li Xiaolan[3], Mao Yuhao[1], Zhang Kuan[1], Ma Xinye[1], Liao Hong[1†]

[1] Jiangsu Key Laboratory of Intelligent Atmospheric Environment Monitoring and Carbon–Pollution Co-control /Jiangsu Collaborative Innovation Center of Atmospheric Environment and Equipment Technology, School of Environmental Science and Engineering, Nanjing University of Information Science and Technology (NUIST), Nanjing 210044, China.

[2] National Meteorological Centre, China Meteorological Administration, Beijing, 100081, China.

[3] Institute of Atmospheric Environment, China Meteorological Administration, Shenyang, Liaoning, 110166, China/Shenyang Academy of Agricultural and Ecological Meteorology, Chinese Academy of Meteorological Sciences, Shenyang 110166, P. R. China

Corresponding author:

Liu Zhenxin (liuzhenxin@nuist.edu.cn) and Liao Hong(hongliao@nuist.edu.cn)

S1 Sensitivity experiments of fractal dimension over North China

S1.1 Experimental setup

Based on the North China case in the main text (24–27 November 2018), near-surface extinction coefficients were calculated at three selected times (25 November 00:00 and 12:00, and 26 November 00:00) for $\mathrm{D_f} = \mathbf{3.0, 2.7, 2.4, 2.1}$ and 2.1, respectively, and the corresponding AOD and VIS were further derived.

Among these, $\mathrm{D_f} = \mathbf{2.4}$ and $\mathrm{D_f} = \mathbf{2.1}$ are the sensitivity experiment settings for $\mathrm{D_f}$ performed in response to the commenter's request. They can also be regarded as extreme hypothetical scenarios in which the aging mechanism of black carbon aerosols is abruptly weakened.

S1.2 Sensitivity results of AOD

The AOD increases significantly as D_f decreases. The AOD at $D_f = 2.1$ far exceeds the reasonable range of observations, demonstrating that D_f is a key parameter controlling AOD.

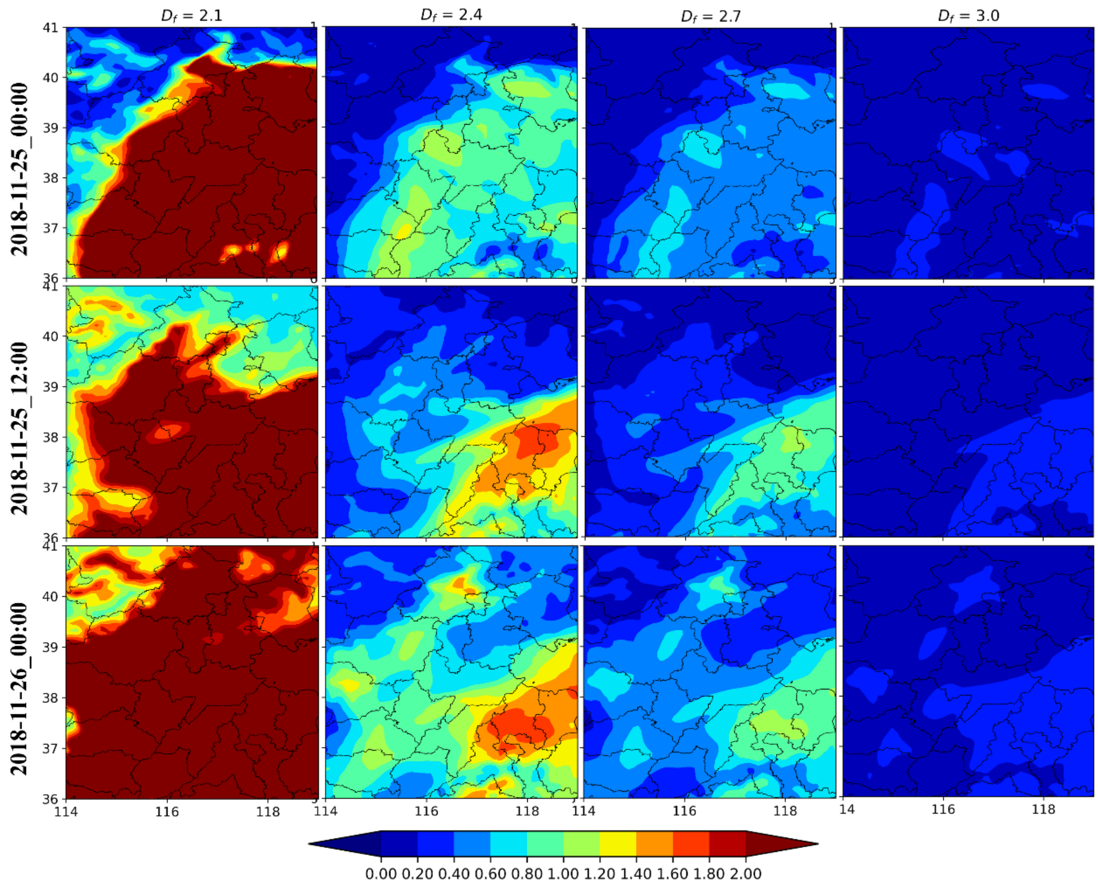

Figure S1: Spatial distribution of AOD over North China at three selected times for D_f = 3.0,2.7,2.4,2.1.

S1.3 Sensitivity results of VIS

The VIS decreases sharply as D_f decreases. The VIS at $D_f = 2.1$ is far lower than the observations, demonstrating the strong sensitivity of visibility simulations to D_f. Meanwhile, the results for $D_f = 2.7$ agree most closely with the observations, indicating that it is a reasonable choice.

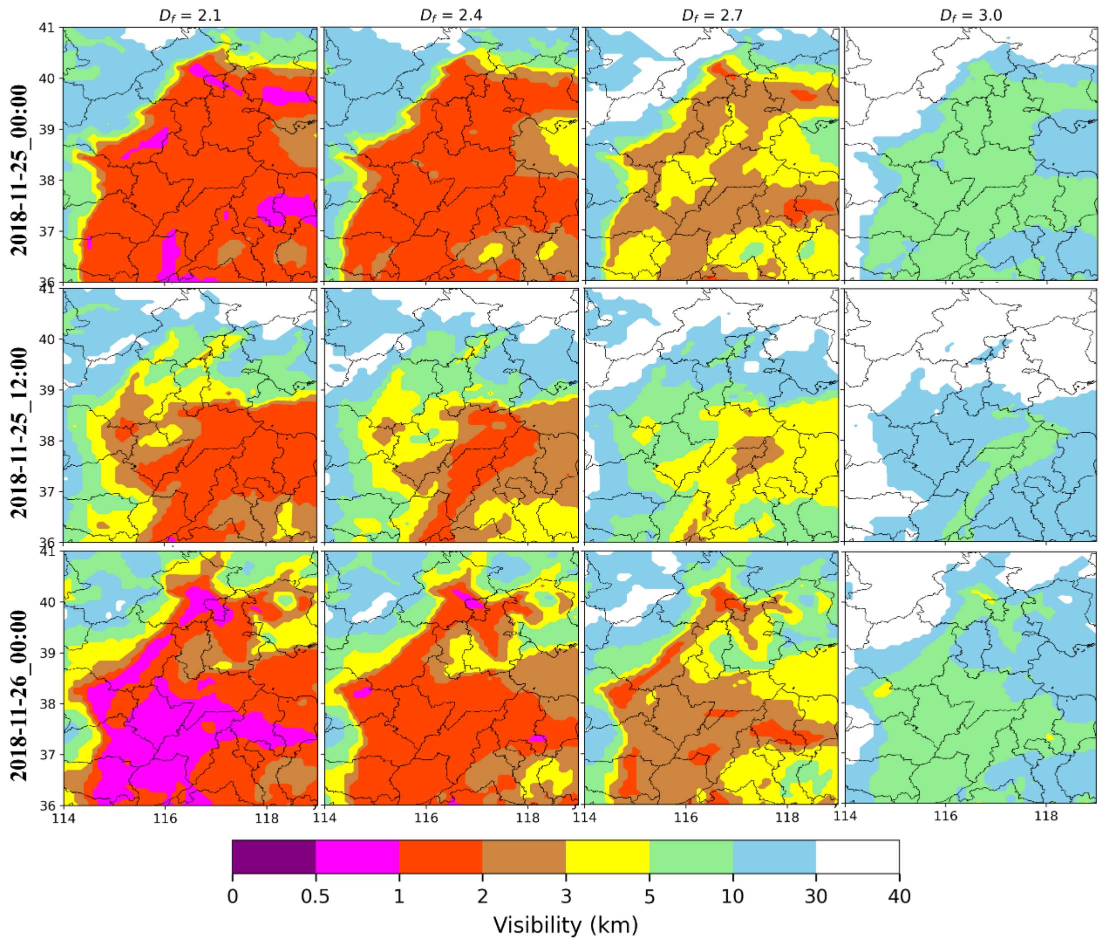

Figure S2: Spatial distribution of near-surface VIS over North China at three selected times for different D_f values, using the same discrete color scale as in the main text.

S1.4 Summary

The main findings of the sensitivity experiments are summarized as follows: (1) D_f exerts a strong control on both AOD and VIS; (2) $D_f = 2.1$ represents unaged fresh soot, and aging processes in the real atmosphere shift it toward 3; (3) $D_f = 2.7$ is a reasonable approximation after aging for the winter haze events over the North China Plain.

S2 Sensitivity experiments of FACM over East Asia

S2.1 Brief description of the model setup

To evaluate the applicability of FACM at a larger spatial scale, an additional set of sensitivity experiments was conducted over East Asia. The simulation domain covers the East Asian continent and adjacent seas, using a single nested grid with a horizontal resolution of 25 km, for the period from 1 to 31 December 2019.

The experimental design follows that of the North China case in the main text, consisting of a control group (CTR, original WRF-Chem) and an experimental group (EXP, WRF-Chem coupled with FACM). Both experiments use identical meteorological initial and boundary conditions and identical physical and chemical parameterization schemes; only the treatment of the equivalent radius in the aerosol optical module differs. The meteorological initial and boundary conditions are taken from the NCEP FNL reanalysis data; anthropogenic emissions are from the MEIC inventory, biogenic emissions from MEGAN, and biomass burning emissions from FINN, while the chemical initial and boundary fields are from CAM-chem output. The physical and chemical schemes include: RRTMG longwave/shortwave radiation, RADM2/SORGAM aerosol chemistry, RADM2 gas-phase chemistry, Fast-J photolysis, Purdue Lin microphysics, Grell 3D cumulus, MYNN2 boundary layer, and Noah land surface processes. It should be noted that this part focuses on evaluating the qualitative impact of FACM at the East Asian scale, and no station-by-station quantitative validation was performed over East Asia; the quantitative validation has already been completed for the North China, Tianjin, and Shenyang cases in the main text.

S2.2 AOD results over East Asia

The high-AOD regions are mainly located over the Central Asian deserts and northern India. The Kyzylkum, Karakum, and Taklamakan deserts in Central Asia are the main sources of dust aerosols; the high AOD over northern India is associated with substantial anthropogenic combustion emissions (black carbon and soot) as well as mixing with dust from the Thar Desert. The AOD simulated by EXP over Central Asia and northern India is generally greater than 0.4, locally approaching 1.0, whereas the maximum AOD in CTR does not exceed 0.5. Over other parts of the East Asian continent, the AOD in EXP is also about 0.1 higher than in CTR, and a local high-AOD feature appears in the South China–Taiwan region. The difference map indicates that CTR overall underestimates AOD, especially over northern India and Central Asia, where the AOD in EXP is about 100%–150% higher than in CTR. This suggests that FACM is more sensitive to the extinction enhancement of non-spherical aerosols with pronounced fractal characteristics, such as dust and carbonaceous aerosols.

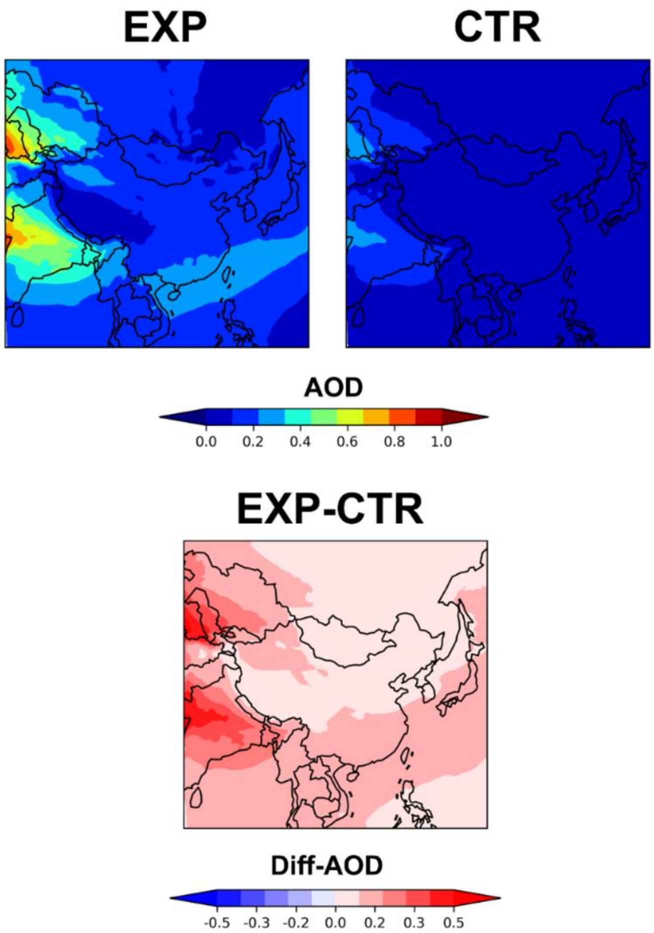

Figure S3: Simulated average AOD over East Asia in December 2019 from EXP and CTR, and their difference (EXP−CTR).

S2.3 SWD and Qcl results over East Asia

The SWD differences between EXP and CTR are mainly concentrated over northern India, the Central Asian deserts, and the South China–Taiwan region, reaching about 20 W m^{-2} over northern India. These regions coincide closely with the high-AOD areas, indicating that enhanced aerosol extinction directly reduces the shortwave radiation reaching the surface. The SWD difference peak over the South China – Taiwan region overlaps with the positive Qcl difference area, suggesting that the reduced SWD in this region may be partly related to increased cloud water. When fractal aerosols act as cloud condensation nuclei, their complex aggregate structures may alter the initial morphology and growth process of cloud droplets, thereby affecting cloud amount and radiative transfer. Over oceanic regions, both AOD and SWD differences are small, consistent with the fact that marine aerosols tend to become spherical after hygroscopic growth and thus exhibit weak fractal effects.

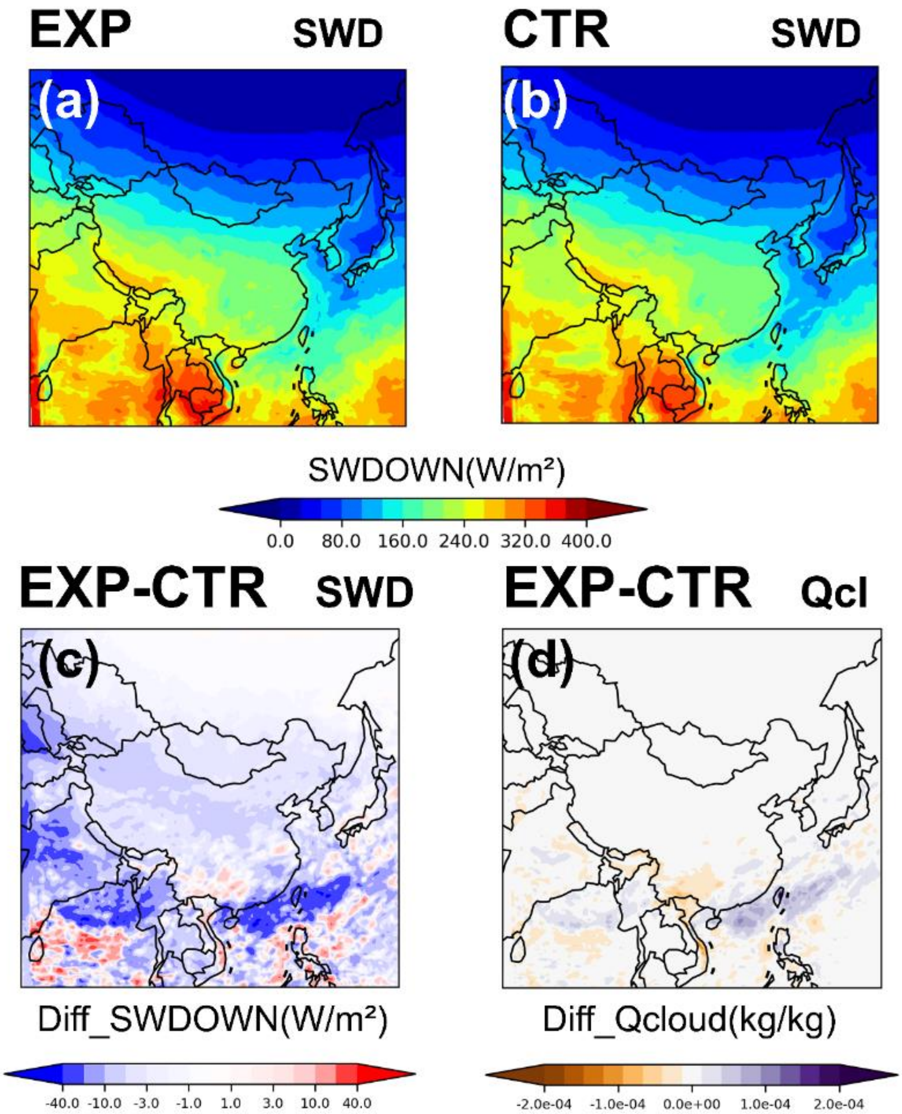

Figure S4 Simulated average SWD and Qcl over East Asia from EXP and CTR, and their differences.

S2.4 TSK results over East Asia

The TSK simulated by EXP is overall lower than that by CTR, especially over the Central Asia–India region and near Sakhalin Island in Outer Northeast Asia, with an average decrease of more than 0.5 °C over Central Asia and India; over the ocean, the difference between the two is close to zero.

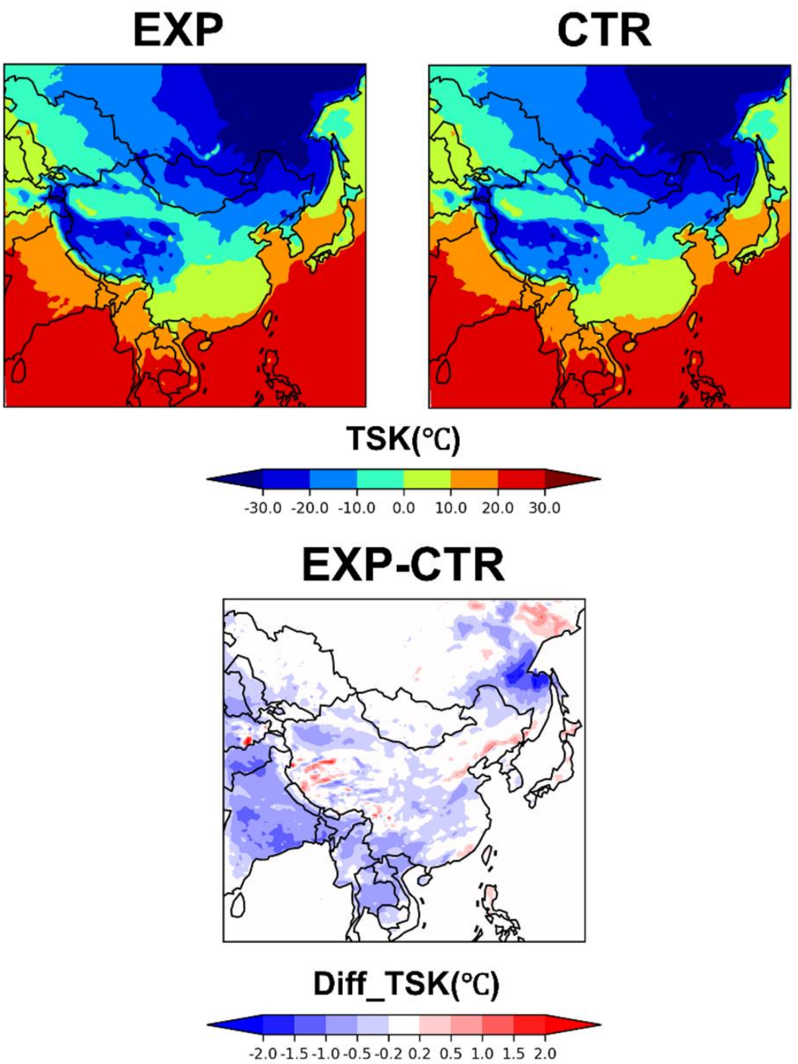

Figure S5: Simulated average TSK over East Asia from EXP and CTR, and their difference.

S2.5 AOD–SWD correlation analysis

After screening for clear-sky daytime conditions with AOD > 0.2, i.e., aerosol-dominated conditions, ΔAOD and ΔSWD are mainly negatively correlated, approaching −1.0 over parts of Central Asia and northern India. This indicates that fractal aerosols intensify the attenuation of shortwave radiation by enhancing scattering and absorption.

S2.6 AOD–TSK correlation analysis

The correlation between ΔAOD and ΔTSK exhibits regional differences: over the Central Asian deserts, where scattering dust dominates, an increase in AOD leads to surface cooling (negative correlation); over northern India and North China, where absorbing aerosols (such as black carbon) account for a relatively high proportion, the fractal characteristics enhance atmospheric heating and indirectly lead to surface warming (positive correlation) by suppressing convection or increasing downward longwave radiation. This indicates that the radiative effect of fractal aerosols depends on regional aerosol chemical composition and geographical environment.

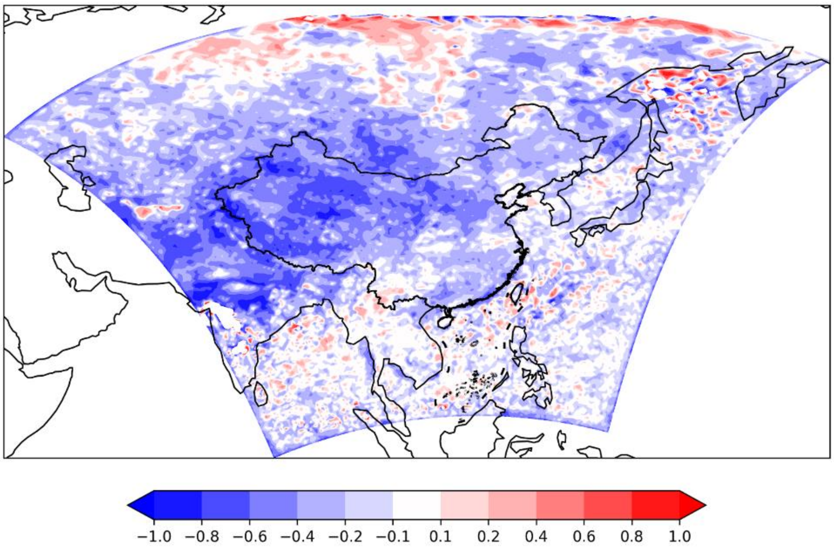

Figure S6: Spatial distribution of the correlation between the AOD difference and the SWD difference from EXP and CTR.

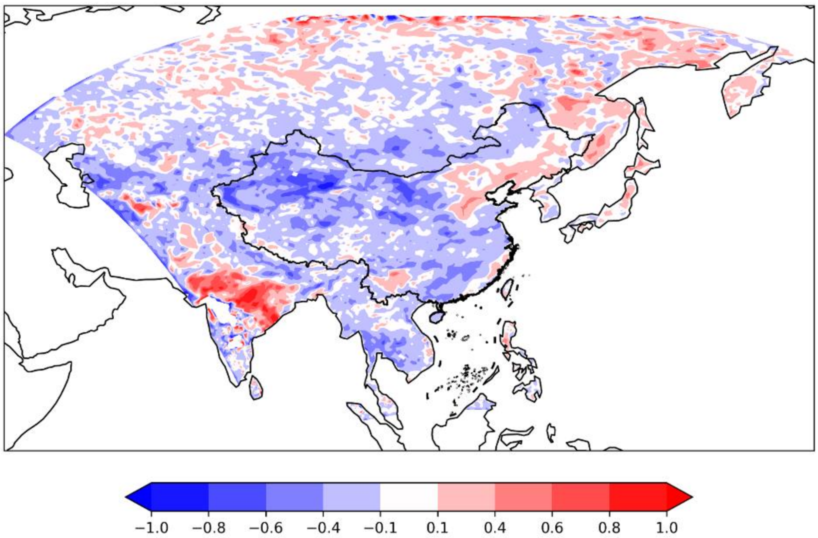

Figure S7: Spatial distribution of the correlation between the AOD difference and the TSK difference from EXP and CTR.

S2.7 Summary

The East Asian sensitivity experiments show that FACM can still capture the significant effects of fractal aerosols on AOD, SWD, and TSK at a larger spatial scale, verifying its transferability and its potential for improving aerosol radiative forcing estimates in GCMs.

S3: Diffusion-Limited Aggregation (DLA) algorithm along with MATLAB scripts for model visualization (Text S1);

The DLA algorithm employed in this study consists of three main components. The first part is the main program body, the function fractal_growth_rad, which simulates the complex and irregular shapes of aerosol clusters as described in section 2.1 of the paper. Additionally, the algorithm calculates the fractal dimension and invokes other functions for the purpose of visualization.

The main part of the DLA algorithm

```
function structure = fractal_growth_rad(N)
    % The size of three-dimensional space
    gridSize = 100;
    % Initialize the three-dimensional space
    structure = zeros(gridSize, gridSize, gridSize);
    origin = [ceil(gridSize/2), ceil(gridSize/2), ceil(gridSize/2)];

    % Place a fixed particle at the origin at the beginning
    structure(origin(1), origin(2), origin(3)) = 1;

    % Define the neighborhood: Use a spherical neighborhood with a radius of 1.5
    neighborOffsets = create_spherical_neighbors(1.5);

    % Initialize the plot
    figure;
    axis equal;
    hold on;
    view(3);
    xlim([0 gridSize]);
    ylim([0 gridSize]);
    zlim([0 gridSize]);
    title(['Dynamic Fractal Aerosol Cluster Growth. N=',num2str(N)]);

    % Add global light sources
    light('Position', [1 1 1], 'Style', 'infinite');
    light('Position', [-1 -1 -1], 'Style', 'infinite');

    draw_sphere(origin(1), origin(2), origin(3), 1);
```

```
    %  Random walk and build the structure
    for i = 1:N
        %  Randomly generate a particle initially¤„
        particlePos    =    origin    +    randi([15,    gridSize/2],    1,
3).*sign(rand(1, 3) - 0.5);

        while true
            % Randomly walk to an adjacent grid point
            step     =     neighborOffsets(randi(size(neighborOffsets,
1)), :);
            particlePos = particlePos + step;

            % If it goes out of bounds, randomly generate the particle
again
            if any(particlePos <= 1) || any(particlePos >= gridSize)
                particlePos  =  origin  +  randi([15,  gridSize/2],  1,
3).*sign(rand(1, 3) - 0.5);
                continue;
            end

            % Check if it is near an existing structure
            for j = 1:size(neighborOffsets, 1)
                neighborPos = particlePos + neighborOffsets(j, :);
                if      structure(neighborPos(1),      neighborPos(2),
neighborPos(3)) == 1
                    % Calculate the distance to the origin¦»
                    distToOrigin = norm(particlePos - origin);

                    %  Calculate  a  fixed  probability  based  on  the
distance
                    fixationProb  =  0.01  +  3.99  *  (distToOrigin  /
(gridSize/2));

                    % particle fixed?
                    if rand < fixationProb
                        structure(particlePos(1),       particlePos(2),
particlePos(3)) = 1;
                        % Dynamically draw the newly grown particle
                        draw_sphere(particlePos(1),     particlePos(2),
particlePos(3), 1.0);
                        drawnow;
                        pause(0.001);
                        break;
                    end
```

```
            end
        end
        if        structure(particlePos(1),        particlePos(2),
particlePos(3)) == 1
            break; % The particle is fixed, stop this random walk
        end
    end
end

% Calculate the fractal dimension - Box Counting Method
boxCounts = [];
boxSizes = 2.^(0:5);
for boxSize = boxSizes
    numBoxes = ceil(gridSize / boxSize);
    boxCount = 0;
    for x = 1:numBoxes
        for y = 1:numBoxes
            for z = 1:numBoxes
                xRange = (x-1)*boxSize+1:min(x*boxSize, gridSize);
                yRange = (y-1)*boxSize+1:min(y*boxSize, gridSize);
                zRange = (z-1)*boxSize+1:min(z*boxSize, gridSize);
                if any(any(any(structure(xRange, yRange, zRange))))
                    boxCount = boxCount + 1;
                end
            end
        end
    end
    boxCounts = [boxCounts, boxCount];
end

% Fit the relationship between box size and box count to calculate
the fractal dimension
logBoxSizes = log( 1./boxSizes);
logBoxCounts = log(boxCounts);
fractalDim = polyfit(logBoxSizes, logBoxCounts, 1);

% Display the fractal dimension
fprintf('Fractal Dimension: %f\n', fractalDim(1));
disp(['Fractal Dimension=', num2str(fractalDim(1))])
% Plot the box counting graph
figure;
scatter(logBoxSizes, logBoxCounts, 'filled');
hold on;
```

```
    % Add the fitted line
    fittedLine = polyval(fractalDim, logBoxSizes);
    plot(logBoxSizes, fittedLine, 'r--', 'LineWidth', 2);

    xlabel('log(1/Box Size)');
    ylabel('log(Box Count)');
    title('Box Counting Method: Fractal Dimension');
    hold off;
end
```

Meanwhile, to ensure the normal operation of the main program, we have also constructed a function function neighborOffsets. Its purpose is to create a spherical neighborhood.

Create a spherical neighborhood.

```
function neighborOffsets = create_spherical_neighbors(radius)
    [x,     y,     z]     =     ndgrid(-ceil(radius):ceil(radius),     -
ceil(radius):ceil(radius), -ceil(radius):ceil(radius));
    distances = sqrt(x.^2 + y.^2 + z.^2);

    % Select points within the spherical radius, but not including
the origin itself.
    valid = (distances <= radius) & (distances > 0);
    neighborOffsets = [x(valid), y(valid), z(valid)];
end
```

Furthermore, we use the function draw_sphere to plot the clusters, making them more visually intuitive.

Plotting the spatial structure of fractal clusters.

```
function draw_sphere(x, y, z, r)
    % Draw a sphere with a 3D grayscale gradient effect at the
specified position with radius r
    [sx, sy, sz] = sphere(50);
    sphereX = r * sx + x;
    sphereY = r * sy + y;
    sphereZ = r * sz + z;
    colormap(gray);
    % Generate a grayscale color matrix, using normalized values of
the 3D coordinates for the grayscale gradient
    C = sqrt(sx.^2 + sy.^2 + sz.^2); % Generate grayscale using
normalized distance from the center of the sphere on the surface
    % Plot the sphere with a grayscale gradient
    surf(sphereX,  sphereY,  sphereZ,  C,  'FaceColor',  'interp',
'EdgeColor', 'none', 'FaceLighting', 'gouraud');
```

```
end
```

S4. Time series plots of visibility simulations and observations at different stations (Figure S8)

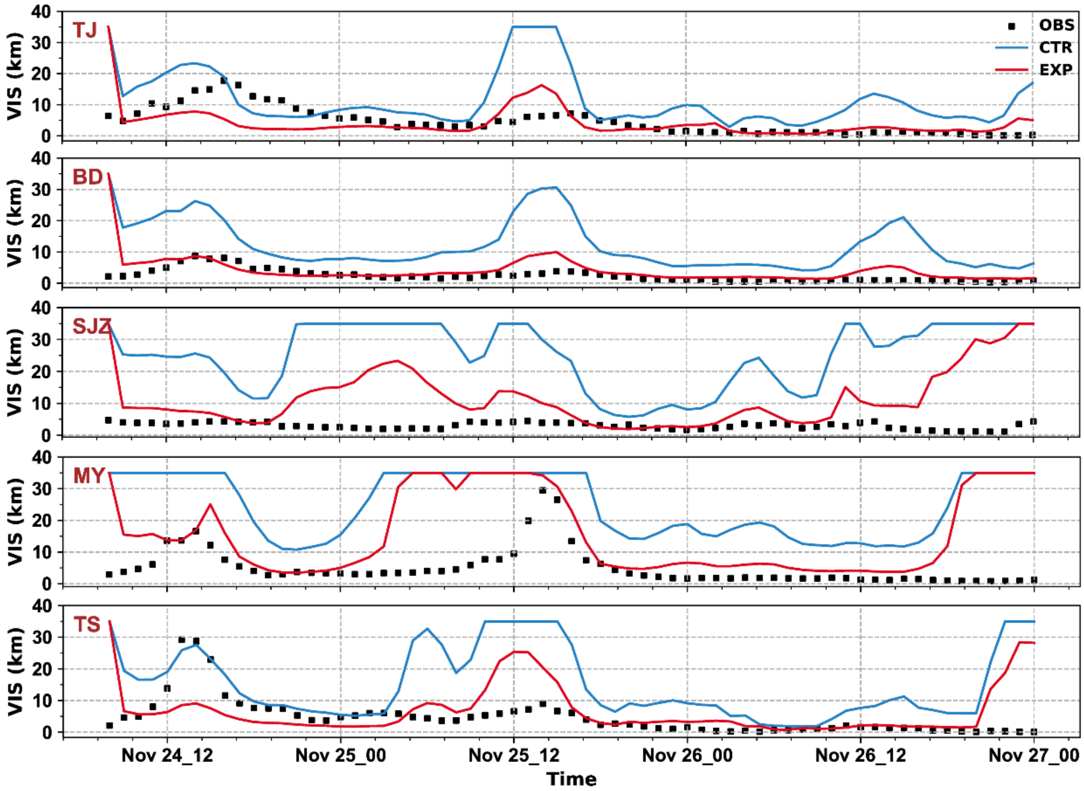

Figure S8. The AV timeseries at station TJ, BD, SJZ, MY and TS: the black square markers (OBS) represent the observation; the blue line (CTR) stands for other by CTR and the red line (EXP) by EXP simulation.

S5. Dependence of the optical-to-aerodynamic radius ratio on fractal dimension and cluster size

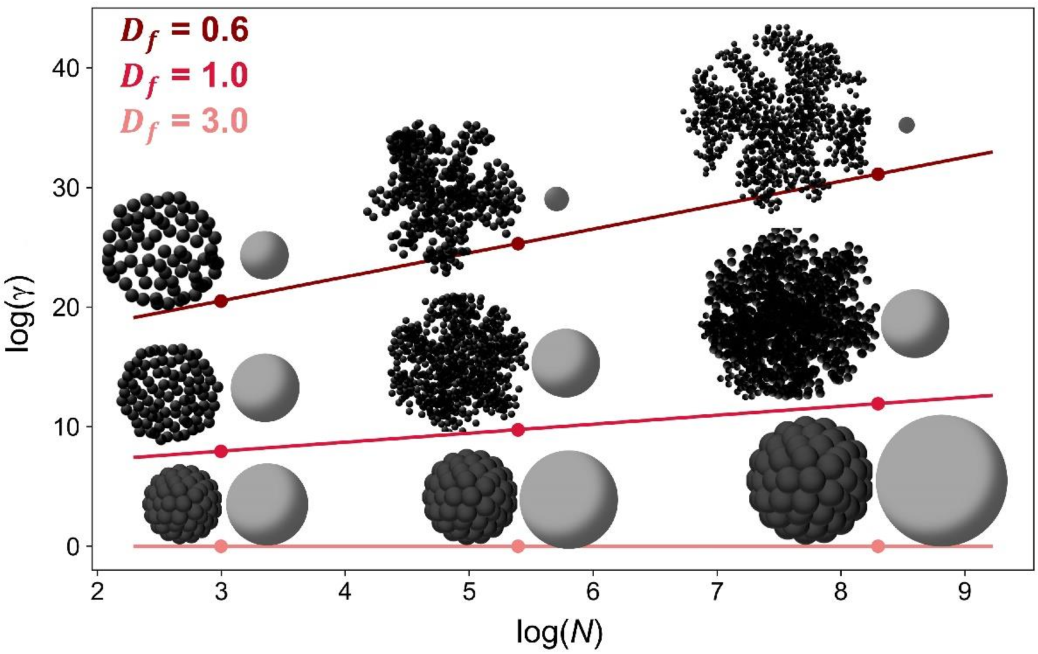

Figure S9. monomer number $\log(N_S)$ and fractal dimension D_f versus $\log(\gamma)$. The different color intensity of solid lines represents different fractal dimensions D_f. The black markers and their sizes represent for the aerosol cluster and its optical equivalent radius. While the gray markers represent for those aerodynamical spherical equivalent radii.

According to Fig. S2 (Figure 2 in the previous draft) we show the most intrinsically different feature of fractal clusters compared to previous aerosol particles with a default dimension of 3: i.e., as the aerosol size (N) grows, the optically equivalent radius of the clusters grows faster than the aerodynamically equivalent radius and the ratio γ of the two is not a linear factor, but rather there is a power-law difference, which is related to the cluster's fractal geometry feature: the fractal dimension of the cluster: D_f. The further D_f deviates from 3, the larger the value of log γ, i.e., a cluster with a smaller aerodynamic equivalent radius also has a stronger optical equivalent radius, which results in a stronger atmospheric scattering signature.

Exceptionally, when D_f is smaller than 1 (a situation that holds only in theoretical derivations, and no such exaggerated examples seem to have been confirmed to have been found in the current sampling observations), it is even possible to have a situation in which the optically equivalent radius of a cluster grows rapidly as the monomers continue to coalesce while the aerodynamically equivalent radius decreases at the same time.

The relevant theoretical derivation is in Sec.2.2 of the manuscript.